Multiphoton excitation and decay processes in xenon: Off-breakdown and breakdown emission at densities up to 1.4×10^{21} atoms cm^{-3}

N. Damany, P. Laporte, J.-L. Subtil, and H. Damany
Equipe de Spectroscopie du Centre National de la Recherche Scientifique, Université Claude Bernard (Lyon I) et Université de Saint-Etienne, 158bis Cours Fauriel, 42023 Saint-Etienne Cédex, France
(Received 10 May 1985)

Spectral, temporal, and density behavior of dye-laser-excited dense xenon below and above breakdown threshold has been studied. Observation of three-photon resonant excitation at 147 nm is limited to very low density ($\rho<7\times10^{16}$ atoms cm^{-3}), whereas four-photon enhanced photoionization plays a major role between 500 mbar and 15 bar of pressure (1.4×10^{19} to 40×10^{19} atoms cm^{-3}). Excitation and deexcitation schemes are discussed from existing data and our spectral and temporal results obtained from either excimer (172-nm continuum) or laser spark emission.

I. INTRODUCTION

Many papers dealing with laser excitation of rare gases have appeared in recent literature. These works were focused on fluorescence, multiphoton ionization or third-harmonic generation but, to our knowledge, the density range was rather limited and little attention has been paid to what happens near the breakdown threshold. The aim of the present paper is to bring new information about xenon behavior in a wide range of density, when excited by a tunable dye laser of moderate power, including the spectral and temporal dependence of excitation below and above the breakdown threshold.

II. EXPERIMENTAL SETUP

The experimental set up (Fig. 1) comprises a modified Sopra tunable dye laser, equipped with improved oscillator and amplificator dye cells,[1] giving a spectral width of 0.01 nm. The dye (Coumarin-120) is pumped by a homemade nitrogen laser, delivering 4 mJ in a 5-ns pulse. The available tunable energy reaches 500 μJ per shot at the center of the 429—454-nm dye fluorescence band. Wavelength calibration is provided by a high-resolution 2.5-m Ebert-Fastie spectrometer. Xenon is contained in a high-pressure cell that can withstand pressure up to 100 bar and is ultra-high vacuum compatible, as well as the gas handling system which includes cold fingers allowing distillation and pressure control of the various gas cycles. The laser beam passes through two in-line silica windows, while the xenon luminescence is observed at a right angle through a side LiF window. In order to minimize self-absorption, the laser beam is focused very near this window by a lens of focal length 86 mm, giving a peak power density of up to $\sim$50 GW cm^{-2} at the center of the $\sim10^{-3}$-cm beam waist.

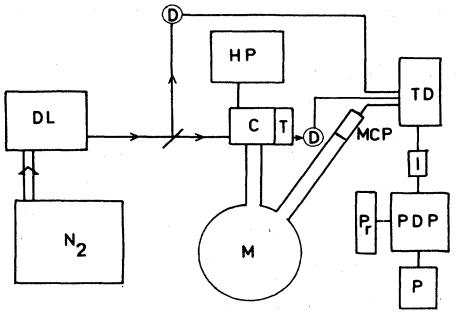

FIG. 1. Experimental setup: N_2 nitrogen laser; DL tunable dye laser; *D* photodiode; *C* Xe cell; HP high-pressure device; *T* temperature control; *M* Seya-Namioka monochromator; MCP microchannel plates; TD Tektronix 7912 fast digitizer; PDP computer; *I* IEEE connection; PR printer; *P* plotter.

The experiments are performed at 25 °C, using a temperature regulation. High-purity xenon from Air Products (99.995% purity) has been used without further purification.

Depending on the experiment, light emission which is limited practically to the beam focus is observed either directly, or through a 40-cm Seya-Namioka monochromator modified in such a way that the light spot acts as the entrance slit. The dispersed light is detected either by a photomultiplier adapted to the investigated spectral range, or by microchannel plates equipped with an additional CsI photocathode:[2] The upper limit of the observed spectral range is consequently 200 nm, whereas the short wavelength cutoff is imposed by the cell window (105 nm).

Signals are analyzed by a fast transient digitizer (Tektronix 7912 AD, rise time 0.7 ns) coupled to a computer (Digital Equipment Corporation PDP11-03). No increase of the rise time is introduced by the additional CsI photocathode.[2] Such a microchannel detector allows detection of signals in a very large intensity range: indeed one is able to record single events, easily detected with the high gain ($\sim10^7$), as well as intense pulses. Depending on the experiments, photomultiplier signals are measured either with a Keithley electrometer coupled to a plotter, or analyzed by the digitizer.

The transmitted laser beam can be detected by a fast photodiode (I.T.L.: rise time 100 ps) coupled to the digitizer.

A proper routine, allowing compatibility between the digitizer and the computer, performs normalization, signal averaging and other data manipulations, final recording, and plotting. The random high-frequency noise as well as the correlated noise induced by the pulsed laser have a typical amplitude of 5 mV (input impedance 50 Ω).

III. EXPERIMENTAL RESULTS

A. Three-photon $6s[\frac{3}{2}]_1^0$ resonance

As a first check, we observed three-photon excitation of the $6s[\frac{3}{2}]_1^0$ state of xenon at low density (10^4 atoms cm^{-3}) known from previous observations by Faisal *et al.*[3] and Salamero *et al.*,[4] and which corresponds to the 147.0-nm one-photon transition. At such a density the linewidth is smaller than the laser width, so that the excitation spectrum is typical of the last one.

The apparent lifetime is of the order of 5 ns: this is an upper limit of the spontaneous emission lifetime since no correction is made for radiation trapping.[5] Indeed, for low density, the self-absorption is very reduced in our mounting, so that the measured lifetime is quite in agreement with the 3.6-ns value deduced from the $f=0.27$ oscillator strength of the $6s[\frac{3}{2}]_1^0 \rightarrow {}^1S_0$ transition,[6] or the 3.46 ns directly measured by Matthias *et al.*[7] in one-photon resonance fluorescence.

At increasing density, a dramatic decrease is observed for the signal associated with the three-photon resonance on the $6s$ level; the almost zero signal which is obtained for pressure above 1 mbar (7×10^{16} atoms cm^{-3}) has to be brought together with the observation by other authors of third-harmonic generation[8,9] which inhibits other processes, as confirmed by theoretical studies.[10,11]

We have not performed a systematic observation in that range of density which has been recently investigated in detail by Salamero *et al.*[4]

B. Four-photon resonance

(1) Off-breakdown excitation. At about 500 mbar (1.4×10^{19} atoms cm^{-3}), although no increase of the global luminescence is observed when tuning the laser around three times the wavelength associated with the ${}^1S_0 \rightarrow 6s[\frac{3}{2}]_1^0$ transition, a sharp increase of the signal is observed when tuning at 440.3 nm: this wavelength corresponds exactly to four times that associated with the four photon allowed ${}^1S_0 \rightarrow 4f[\frac{3}{2}]_2,[\frac{9}{2}]_4$ transitions, not resolved here. The spectral analysis of that signal reveals that it corresponds to the well-known second continuum of the Xe_2 centered around 172 nm.

A decay time constant of 85 ns is associated with that signal. At increasing pressure (500 mbar to 10 bar) we observe a decrease of the decay time constant whereas new four-photon resonances appear on the $6p'$ ($\lambda_{laser}=445$ nm), $7p$ (451 nm), $8p$ (434 nm), and $5f$ (428 nm) levels. The decay time constants associated with the different excitations are identical. Figure 2 shows a typical oscillogram of the fluorescence of Xe at a density of 5.4×10^{19} atoms cm^{-3} (2 bar). Above 2.5 bar, the laser power has to be reduced to follow the behavior of the resonances without getting breakdown.

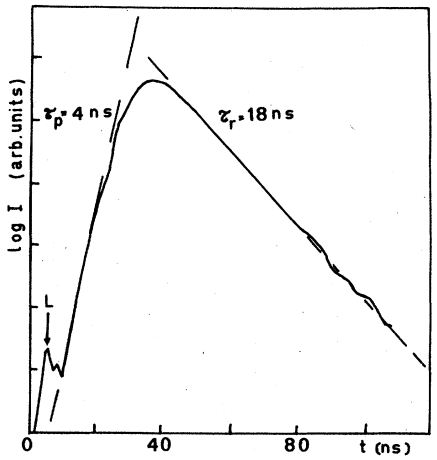

FIG. 2. Typical decay of global xenon luminescence. $\rho_{Xe}=2$ amagats (5×10^{19} atoms cm^{-3}), $E_1=300$ μJ.

(2) Breakdown excitation. Above 2 bar, it was possible, with the available power, to induce the breakdown selectively. Its occurrence is characterized by an increase of the emission by several orders of magnitude, so that direct analogic traces from the electrometer can be obtained, as presented in Fig. 3, for several xenon densities. This figure illustrates the density dependence of the spectral selectivity; in particular, it shows that, at increasing density, breakdown may occur at increasing spectral distance from the three-photon resonance on the $6s$ level, acting as inter-

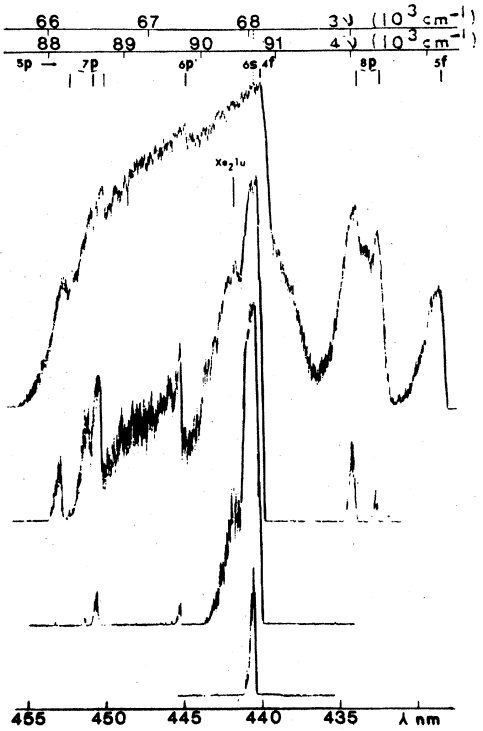

FIG. 3. Breakdown excitation spectrum of xenon: Xe density (from bottom to top): 5, 6, 6.5, and 8 amagats.

mediate level; so four-photon resonances are successively observed on levels: $4f[\frac{5}{2}]_2$ and $[\frac{7}{2}]_4$ ($\lambda_1=440.2$ nm), $4f[\frac{5}{2}]_2$ ($\lambda_1=439.9$ nm), $4f[\frac{7}{2}]_4$ ($\lambda_1=439.8$ nm) (Fig. 4); $6p'[\frac{1}{2}]_0$ ($\lambda_1=445.2$ nm); $7p[\frac{1}{2}]_0$ ($\lambda_1=450.4$ nm), $7p[\frac{3}{2}]_2$ ($\lambda_1=451.2$ nm) $7p[\frac{5}{2}]_2$ ($\lambda_1=452.9$ nm); $8p[\frac{5}{2}]_2$ ($\lambda_1=434.6$ nm), $8p[\frac{1}{2}]_0$ ($\lambda_1=433.0$ nm), and $5f$($\lambda_1=428.4$ nm).

It is, to our knowledge, the first direct evidence of a resonant multiphoton breakdown initiation. It rules out the hypothesis of some impurity effect or naturally occurring free electrons.

An increase of laser energy at fixed xenon density, as well as an increase of density at fixed laser energy, gives rise to broadening and overlapping in the excitation spectrum. Only the density effect has been systematically studied because of energy limitation of the laser. For densities above 2.7×10^{20} atoms cm^{-3} a large overlapping is observed; at 5×10^{20} atoms cm^{-3} the spectral selectivity of the excitation disappears totally and breakdown is easily obtained, from the same typical laser energy, in the range 473 to 547 nm (C 307 dye), which corresponds to a large detuning.

C. Rise and fall of the breakdown

Experiments on breakdown threshold and spectral or temporal properties of its light emission have also been performed. For these experiments, the laser wavelength was fixed at 440 nm, which is the more efficient at relatively low pressure, when the selectivity of excitation has not totally disappeared.

(1) Breakdown threshold. Though the quality of the transmitted laser beam could be severely affected as soon as the breakdown occurs, especially at high density, the time-resolved signal (Fig. 5) allows us to determine the instant when the strong absorption characterizing the breakdown occurs and the corresponding laser intensity I_{th}. In Fig. 6 we have plotted in a log-log scale I_{th} versus xenon density. Experimental points stand on a straight line with gradient -0.96, a result which will be discussed later.

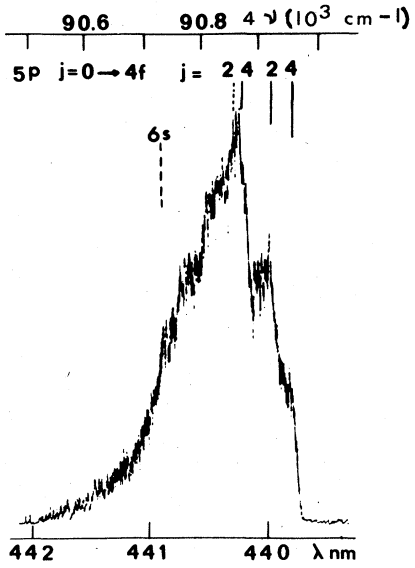

FIG. 4. High-resolution breakdown excitation spectrum of xenon near the $4f$ resonance: Xe density 4.9 amagats.

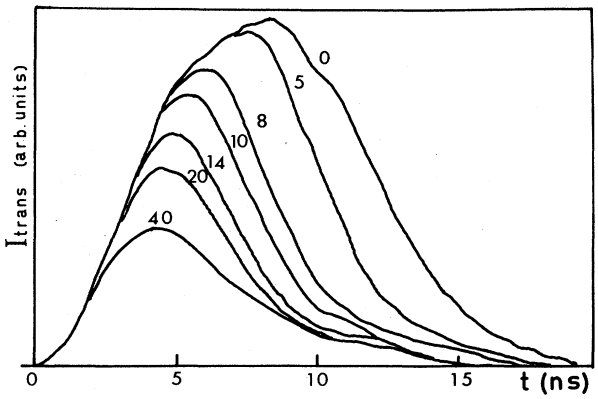

FIG. 5. Intensity of the transmitted laser beam for various Xe densities (density in amagat unit: 1 amagat$=2.7\times10^{19}$ atoms cm^{-3}): $E_1=350$ μJ.

(2) Spectrum of the light emitted by the xenon breakdown. When spectrally analyzed with the monochromator, the light emitted from the bright spot associated with the breakdown ("laser spark") appears as a broad continuum extending from the visible towards the vuv down to the Xe resonance lines at 147 and 129.5 nm, for which a strong self-absorption takes place. Blurred structures, especially around 230 and 250 nm suggest the presence of pressure broadened Xe II and Xe III lines. This emission is quite similar to that reported by Silfvast *et al.*[12] for both laser-produced and dc-heated plasmas.

(3) Intensity of the laser spark emission. We have followed the dependence of the laser spark emission, observed in the zeroth order of the monochromator, with xenon density at fixed laser energy and with laser energy at fixed xenon density. In spite of the spectral limitation of the receptor, it is expected that the observed behavior is that of the global emission.

Figure 7 presents the typical xenon density dependence in the range 7.8×10^{19} atoms cm^{-3} to 1.65×10^{21} atoms cm^{-3} for which the breakdown was obtained with the laser energy chosen. Clearly the intensity increases steeply from a threshold density near 7×10^{19} atoms cm^{-3} up to a density of 27×10^{19} atoms cm^{-3} for which it reaches a maximum and then decreases; a high-density

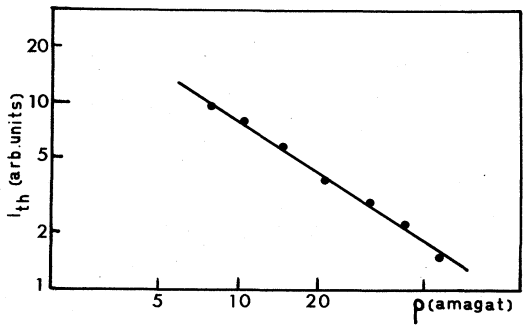

FIG. 6. Laser intensity at breakdown threshold vs xenon density, in log-log scale; slope of the straight line is -0.96.

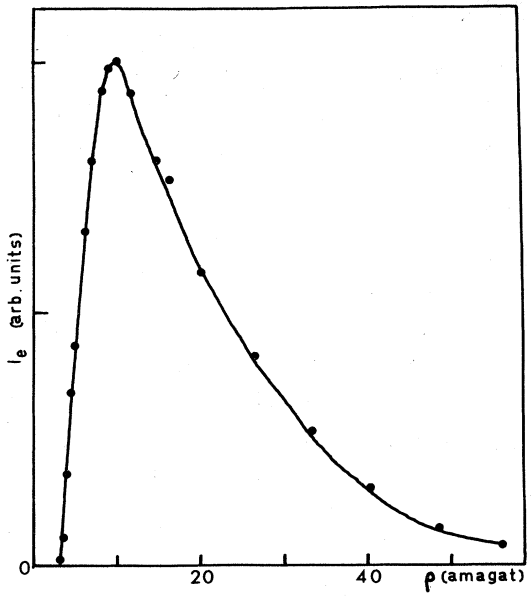

FIG. 7. Intensity of the laser spark emission vs xenon density: $E_1 = 350\ \mu J$.

threshold appearing at about 160×10^{19} atoms cm^{-3}. Maximum and threshold densities vary slightly with the experimental conditions but the intensity versus density curves remain very similar. The variation of total radiance at constant density ($\sim 7 \times 10^{20}$ atoms cm^{-3}) as a function of the laser input energy is shown in Fig. 8.

(4) Temporal behavior of the spark emission. Figure 9 gives a typical example of the temporally resolved spark emission. When the observation is performed at a wavelength totally outside the 172-nm excimer fluorescence, a monotonous decay is obtained which is attributed to the plasma thermalization. As for the $\lambda = 172$-nm curve, it reveals a fast component followed by a slower one whose decay rate is quite identical to the other curve. We ascribe the fast component to the decay via the 0_u^+ excimer state of all the excited neutral states created during the laser ac-

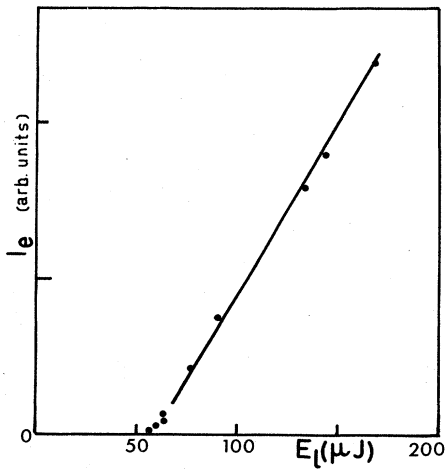

FIG. 8. Intensity of the laser spark emission vs laser energy: $\rho_{Xe} = 26$ amagats (7×10^{20} atoms cm^{-3}).

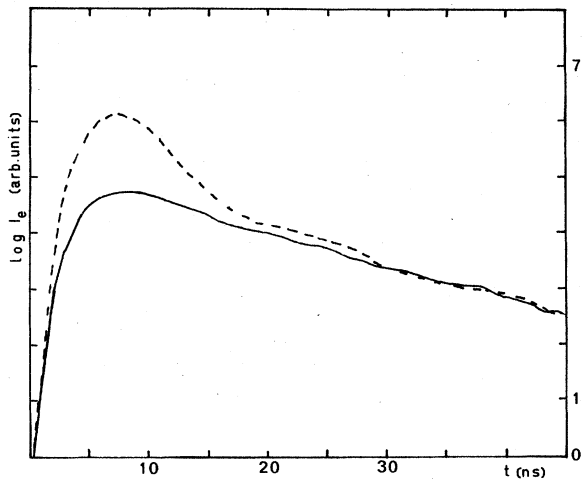

FIG. 9. Typical decay of the laser spark emission. Dashed line: $\lambda_{obs} = 172$ nm; solid line $\lambda_{obs} = 140$ nm; final time constant: 18 ns.

tion, then followed by ionic recombination which is regulated by the thermalization process. As the involved processes are much too dependent on the excitation conditions, no other spectral or density dependence of the temporal behavior has been looked for.

IV. DISCUSSION

Although processes are very different whether breakdown occurs or not, the involved mechanisms are imbricated and, in particular, the first steps of the excitation are the same in both cases. So, for sake of clarity, we shall separate the discussion into three parts: primary processes of excitation, off-breakdown xenon luminescence, and the rise and fall of the breakdown.

A. Primary processes for excitation

The excitation spectra of luminescence or breakdown will be discussed with the help of the energy diagram of Xe and Xe_2 (Fig. 10) after two preliminary remarks: (i) breakdown development requires the presence of primary electrons; (ii) off-breakdown, Xe_2 (0_u^+) excimer formation is a necessary step as the final luminescence is essentially composed of the well-known second continuum centered at 172 nm.

The ability of exciting by a four-photon process at low density with a rather modest laser energy in a limited spectral region only, can be attributed to an enhancement of the transition probability in the close neighborhood of the resonance on $6s[\frac{3}{2}]_1^0$ atomic state in agreement with other observation.[13] This is also supported by the order of appearance of the four-photon resonances. The fact that increasing density results in easier excitation can be attributed to the broadening of both the excited and the intermediate levels (6) thus enhancing the multiphoton transition probability.

A two-step process, involving three-photon excitation, cannot be retained because of the rather large detuning and, furthermore, because a fast (~ 4 ns) undelayed decay

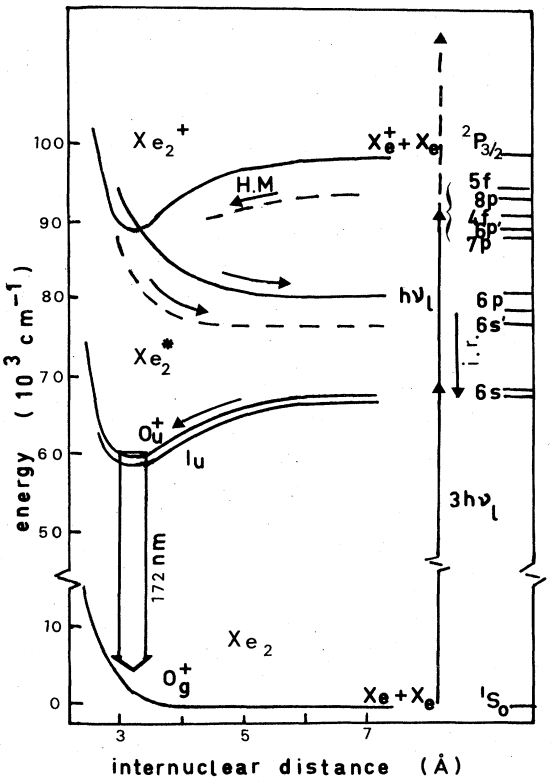

FIG. 10. Simplified energy-level diagram of atomic and molecular xenon illustrating the main decay processes.

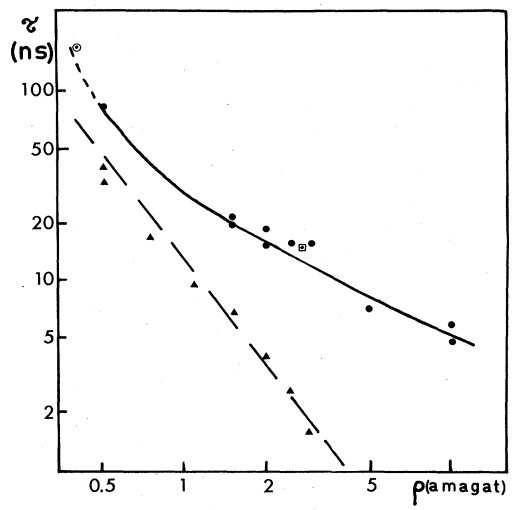

FIG. 11. Production and radiative time constants. Production time constant: ▲, experimental values; dashed line: minus 2 slope (see the text). Radiative time constants: ●, present work; ⊡, Keto *et al.* (Ref. 16); ⊙, deduced from McCown *et al.* data (Ref. 17).

would have been observed since the Xe_2 (0_u^+) excimer formation is very fast in the investigated density range.

Atomic xenon being excited, what is the following step? In sight of our experimental results and of the data of the literature, we may state that molecular ions Xe_2^+ are involved: (i) ion formation is essential to breakdown initiation and, at such densities, if atomic ions were created molecular ions would be formed very quickly due to collisions and associated strongly attractive forces; (ii) at fixed density, we observe the same time behavior for all the four-photon excited levels: as these levels have no chance to have so slow and identical direct decay channels, the observed decay constants have to be related to other processes. Taking these remarks into account, several processes subsequent to the four-photon excitation and producing ions can be proposed,

$$Xe^* + h\nu \rightarrow Xe^+ + e^-;\ Xe + Xe^+ \rightarrow Xe_2^+ , \quad (1)$$

$$Xe^* + Xe \rightarrow Xe_2^+ + e^- , \quad (2)$$

$$Xe_2^* + Xe_2^* \rightarrow 2Xe + Xe_2^+ + e^- , \quad (3)$$

$$Xe_2^* + h\nu \rightarrow Xe_2^+ + e^- . \quad (4)$$

(1) is a five-photon ionization, the molecular ion being the first step of the fast-decay process due to Xe-Xe^+ collisions. (2) is an associative ionization (Hornbeck-Molnar effect). Previous works either in the same density range[14] or at lower density[15] showed that it is a very efficient process, with a time scale $< 10^{-8}$ s, as far as atomic levels with energy above that of the ground-state molecular ion Xe_2^+ are considered. One has also to mention that at such densities, mechanisms associated with band formation may occur, with possible direct four-photon electron release into the conduction band[14] even at energies below the above mentioned limit. (3) Penning ionization resulting from collision between excimers does not seem probable in the present regime. (4) it comes either from a four-photon excitation known to give the ion spontaneously, without an extra photon, or from a three-photon excitation which would give a maximum for $6s[\frac{3}{2}]_1^0$ resonance, with, in fact, two additional photons necessary to get the ion.

As for the question whether a four- or a five-photon process has to be considered, although the answer is not crucial since both lead to the molecular ion, we favor the idea that the four-photon process is dominant, at least at laser intensity for which a signal appears. Indeed, when the breakdown occurs (Fig. 3) intensity drops on the blue side of the associated resonances are observed, which can be understood as a lower probability of creating initial ions when exciting on the repulsive part of the molecular potential curves. In case of a five-photon process such repulsive curves would behave like the attractive ones and the excitation profile would be quasisymmetrical.

B. Off-breakdown xenon luminescence

Starting from the previous considerations, we shall discuss the time behavior of the emission from the well-known low levels of the excimer Xe_2^* (0_u^+ and 1_u molecular states associated, respectively, to $6s[\frac{3}{2}]_1^0$ and $6s[\frac{3}{2}]_2$ atomic levels) (Fig. 11).

On Fig. 11 are plotted, with a log/log scale, the radiative time constant τ_r and the production time constant τ_p as directly evaluated from curves such as on Fig. 2. It is to be noticed that τ_r, which is dependent on gas density, is

not sensitive to the other experimental conditions, particularly to the laser power, which allows us to compare our results to that of other authors.[16,17] On the contrary τ_p depends on laser power and focusing parameters, so that only results obtained in the same conditions can be compared. In spite of the scarcity of experimental results, two striking features are evidenced: the late rise time of the signal at lower pressure and its nearly ρ^{-2} variation with density, which suggests a three-body reaction for the production of the emitting species.

The decay sequence from the molecular ion is now well known: dissociation into a $6p$ excited atom and a $^1S_0$ ground-state atom, $Xe_2^+ \rightarrow Xe$, $6p(\frac{1}{2},\frac{3}{2},\frac{5}{2})+Xe+E_c$, due to the crossing of the related potential-energy curves; radiative decays between $6p$ and $6s$ states, which fall in the near infrared and has not been searched for in the present work, followed by $Xe^* + 2Xe \rightarrow Xe_2^* + Xe$.

McCown[18] has determined a spontaneous emission lifetime of 29 ns for $6p[\frac{1}{2}]_0$ level and a rate constant for two-body quenching of that state of $(4\pm1)\times10^{-10}$ $cm^3 s^{-1}$, so that, even for the lower densities used in our study (10^{19} at cm^{-3}) the corresponding decay constant τ is less than 1 ns. The associated branching ratio is very large at 0.998, as for other $6p$ states.[19]

C. Rise and fall of the breakdown

Schematically, the processes leading to the breakdown are: (i) creation of primary electrons; (ii) gain of energy from the laser beam to produce new ionization, developing a cascade process; (iii) very strong heating by the laser field if a dense enough plasma is created by (ii).

Unambiguously, multiphoton processes are responsible for the primary electrons, but both the involved laser energy and the fact that the observed thresholds or intensities do not approximate a E_{laser}^n ($n=3$ or 4) law, point out that they do not govern the breakdown rise; more probably, a cascade ionization takes place from the primary electrons which get energy from the laser field. At this step, many competing processes are involved: inverse bremsstrahlung, attachment, diffusion, recombination, depending generally on the gas density and/or on the electric field. As a consequence, observed results largely depend on the experimental conditions, and no complete calculation is available (for an extended review see, for instance, Ref. 20).

Calculations and experiments[20–26] concerning the breakdown threshold deal generally with the minimum laser power inducing the breakdown; these results can be transposed directly to the case when the energy of the laser pulse and its duration are largely higher than necessary, as far as we can determine the time when the breakdown occurs and evaluate the corresponding laser intensity.

Assuming that the electron-atom collision frequency is proportional to the gas density ρ, three limiting cases can be considered, corresponding at a rough approximation, to[22]: (i) $I_{\text{th}} \propto \rho^{-2}$ in low-pressure regime, when diffusion is the main loss mechanism, (ii) $I_{\text{th}} \propto \rho^{-1/3}$ if recombination is the main loss mechanism (very high density), (iii) $I_{\text{th}} \propto \rho^{-1}$ if neither recombination nor diffusion is involved.

We find for I_{th} a $\rho^{-0.96}$ dependence (Fig. 6) which suggests that neither diffusion nor recombination is important at the investigated densities. Indeed, any interpretation of the gradient signification is questionable due to the multiplicity of implicated processes in high-radiation field and at high density. Firstly, some multiphoton inverse bremsstrahlung can influence the ionization process, two-step ionization and photoionization of the excited atom taking place.[26] Secondly, self-focusing, refraction, scattering, plasma expansion or constriction in dense medium, can affect the beam intensity at the focal spot in various (and opposite) ways.[20,27–30]

Once the threshold is reached, the plasma becomes strongly absorbing. The absorbed energy is essentially used to heat the gas,[31,32] so that it is not surprising to observe an emission spectrum relatively flat in a large spectral range (if one excepts broadened superimposed emission lines or dips from self-absorption), characteristic of a blackbody radiation. The behavior of the spectral radiance as a function of the laser input (Fig. 7), or of the xenon density (Fig. 8) is qualitatively very similar to that reported by Silfvast[12] in spite of rather different experimental conditions ($\lambda_1=10.6$ μm, instead of $\lambda_1=0.44$ μm). The more striking difference is the density which maximizes the light emission (0.2×10^{19} atoms cm^{-3} in Silfvast work, 3×10^{20} atoms cm^{-3} in the present work) but this difference is not surprising if one considers that energy is absorbed by electrons at a rate which depends both on the frequency of the electric field created by the laser and on the ion-electron collision frequency. Typically, the mean rate of heating of a single electron is[31] $dT_e/dt = R_H - R_{\text{th}} - R_{ei}$ where $R_H \propto eE^2\nu_{ei}/m_e\omega^2$, R_{th} is the term for conduction losses ($\propto 2T_e/\rho$) and R_{ei} that for the losses by electron-ion energy transfer [$\propto (T_e - T_i)\rho/T_e^{3/2}$], where E designs the electric field created by the laser, ω its frequency, and ν_{ei} the electron-ion collision frequency, and T_e and T_i the electronic and ionic temperatures. As the frequency of our dye laser is approximately 24 times higher than that of the CO_2 laser used by Silfvast, we observe the maximum of emission at a pressure very much higher.

V. CONCLUSION

We have systematically studied spectral, temporal, and density dependence of breakdown and off-breakdown laser excitation of xenon. In particular, we were able to give the first direct evidence of resonant multiphoton-induced breakdown in a gas. Associative ionization (Hornbeck-Molnar effect) from the four-photon highly excited atomic states, seems responsible for the initial electron formation. Various observations of the emitted light bring some new informations about the mechanisms involved in highly excited excimer systems.

ACKNOWLEDGMENTS

This work has been partly supported by a special grant from the Centre National de la Recherche Scientifique (A.T.P. No. 8099). The Equipe de Spectroscopie is part of the Laboratoire de Spectrométrie Ionique et Moléculaire which is associated (UA 171) with the Centre National de la Recherche Scientifique.

[1]J.-Y. Roncin and H. Damany, Rev. Sci. Instrum. **52**, 1922 (1981).
[2]P. Moutard, P. Laporte, and H. Damany, Rev. Phys. Appl. **19**, 409 (1984).
[3]F. H. Faisal, R. Wallenstein, and H. Zacharias, Phys. Rev. Lett. **39**, 1138 (1977).
[4]Y. Salamero, A. Birot, H. Brunet, J. Galy, and P. Millet, J. Chem. Phys. **80**, 4774 (1984).
[5]T. Holstein, Phys. Rev. **72**, 1212 (1974).
[6]P. Laporte and H. Damany, J. Phys. (Paris) **40**, 9 (1979).
[7]E. Matthias, R. A. Rosenberg, E. D. Poliakoff, M. G. White, S.-T. Lee, and D. A. Shirley, Chem. Phys. Lett. **52**, 239 (1977).
[8]J. C. Miller, R. N. Compton, M. G. Payne, and W. W. Garrett, Phys. Rev. Lett. **45**, 114 (1980).
[9]J. H. Glownia and R. K. Sander, Phys. Rev. Lett. **49**, 21 (1982).
[10]M. G. Payne and W. R. Garrett, Phys. Rev. A **26**, 356 (1982).
[11]M. Poirier, Phys. Rev. A **27**, 934 (1983).
[12]W. T. Silfvast and O. R. Wood, Appl. Phys. Lett. **25**, 274 (1974).
[13]K. Aron and P. M. Johnson, J. Chem. Phys. **67**, 5099 (1977).
[14]P. Laporte, V. Saile, R. Reininger, U. Asaf, and I. T. Steinberger, Phys. Rev. A **28**, 3613 (1983).
[15]R. Reininger, V. Saile, and P. Laporte, Phys. Rev. Lett. **54**, 1146 (1985).
[16]J. W. Keto, R. E. Gleason, and G. K. Walters, Phys. Rev. Lett. **33**, 1365 (1974).
[17]A. W. McCown, M. N. Ediger, S. M. Stazak, and J. G. Eden, Phys. Rev. A **28**, 1440 (1983).
[18]A. W. McCown, M. N. Ediger, and J. G. Eden, Phys. Rev. A **26**, 2281 (1982).
[19]H. Horiguchi, R. S. F. Chang, and D. W. Setser, J. Chem. Phys. **75**, 1207 (1981).
[20]T. P. Hughes, in *Plasmas and Laser Light* (Hilger, London, 1975) p. 200.
[21]A. V. Phelps, in *Physics of Quantum Electronics,* edited by Kelly *et al.* (McGraw-Hill, New York, 1966) p. 538.
[22]R. W. Minck, J. Appl. Phys. **35**, 252 (1964).
[23]F. Morgan, L. R. Evans, and C. Grey-Morgan, J. Phys. D **4**, 225 (1971).
[24]C. L. M. Ireland and C. Grey-Morgan, J. Phys. D **7**, L87 (1974).
[25]R. J. Dewhurst, J. Phys. D **10**, 283 (1977).
[26]Y. E. Gamal and A. Harith, J. Phys. D **16**, 1901 (1983).
[27]M. H. Key, D. A. Preston, and T. P. Donaldson, J. Phys. B **3**, L88 (1970).
[28]V. V. Korobkin and A. J. Alcock, Phys. Rev. Lett. **21**, 1433 (1968).
[29]V. N. Lugovoi and A. M. Prokhorov, Zh. Eksp. Teor. Fiz. Pis'ma Red. **7**, 153 (1968) [JETP Lett. **7**, 117 (1968)].
[30]S. A. Ramsden and W. E. R. Davies, Phys. Rev. Lett. **13**, 227 (1964).
[31]R. G. Meyerand and A. F. Haught, Phys. Rev. Lett. **11**, 401 (1963).
[32]R. W. Minck and W. G. Rado, J. Appl. Phys. **37**, 355 (1966).